A DISTURBANCE COMPENSATION CONTROL FOR AN ACTIVE MAGNETIC BEARING SYSTEM BY A MULTIPLE FXLMS ALGORITHM

Min Sig Kang

Department of mechanical engineering, Kyungwon University, Sungnam, Kyunggido, KOREA

Joon Lyou

Dept. of Electronics Eng., Chungnam National Univ., Daejeon 305-764, KOREA

Keywords: Active magnetic bearing, Multiple filtered-x least mean square algorithm, Acceleration feedforward compensation

Abstract: In this paper, a design technique is proposed for a disturbance feedforward compensation control to attenuate disturbance responses in an active magnetic bearing system, which is subject to base motion. To eliminate the sensitivity of model accuracy to disturbance responses, the proposed design technique is an experimental feedforward compensator, developed from an adaptive estimation, by means of the Multiple Filtered-x least mean square (MFXLMS) algorithm. The compensation control is applied to a 2-DOF active magnetic bearing system subject to base motion. The feasibility of the proposed technique is illustrated, and the results of an experimental demonstration are shown.

1 INTRODUCTION

Active magnetic bearing (AMB) systems are increasingly used in industrial applications. Unlike conventional bearings, AMB systems utilize magnetic fields to levitate and support a shaft in an air-gap within the bearing stator. When compared to conventional mechanical bearings, AMB offers the following unique advantages: non-contact, elimination of lubrication, low power loss, and controllability of bearing dynamic characteristics.

Recently, interest has increased regarding the application of AMB systems to the sight stabilization systems mounted on moving vehicles. When a vehicle is undergoing angular motion, the mirror axis of sight rotates relative to the vehicle, to stabilize the line of sight. In such systems, the friction of mechanical bearings that support the mirror axis may cause tracking errors and, hence, may deteriorate the quality of an image obtained through electro-optical equipment. To eliminate the undesirable effects of friction, an AMB system is used instead of mechanical bearings.

The main problem of a sight system levitated and stabilized by an AMB is the image scattering caused by base motion. One solution for reducing the effects of base motion is to expand the bandwidth of the control system by using feedback controls (Cole, 1998) such as PID control, state feedback control, H^{∞} control, and so on. A controller with a wider bandwidth, however, requires a higher sampling frequency, which often induces a mechanical resonance.

An alternative approach for disturbance attenuation is a feedforward compensation of the base acceleration. The effectiveness of this approach has been demonstrated in the field of hard disk drives, which are also subject to base motion (Jinzenji, 2001). Suzuki (1998) developed feedforward compensation based on a dynamic model of the AMB system and showed that increases in the vibration rejection can be achieved. In practice, however, a dynamic model is not reliably accurate, because of many problems associated with it, such as the non-linearity of AMB, approximation errors of the discrete equivalent to a continuous transfer function, and sensor dynamics.

Motivated to overcome these problems, in this work an alternative technique is proposed: a non-model based acceleration feedforward compensation control developed from an adaptive estimation, by means of the multiple filtered-x least mean square

Kang M. and Lyou J. (2004).
A DISTURBANCE COMPENSATION CONTROL FOR AN ACTIVE MAGNETIC BEARING SYSTEM BY A MULTIPLE FXLMS ALGORITHM.
In *Proceedings of the First International Conference on Informatics in Control, Automation and Robotics*, pages 264-269
DOI: 10.5220/0001135102640269

(MFXLMS) algorithm (Kuo, 1996; White, 1997). The performance and the effectiveness of the proposed technique are demonstrated on a 2-DOF AMB system subject to base motion.

2 SYSTEM MODEL

The test rig used in this paper is an AMB system of 2-DOF shown in Fig. 1. Figure 2 is the photograph of the test rig. The test rig consists of two sets of AMB(left AMB: AMB-1, right AMB:AMB-2) and a circular shaft. Each end of the shaft is tied up by string wire such that the shaft moves only in the vertical plane. Each electromagnet is attached rigidly to each shaker(B&K-4808), which generates base motion resembling the vehicle motion. Two non-contacting proximity displacement sensors(AEC-5505) measure each air gap between the probe tip and the shaft surface, and the vertical acceleration of each electromagnet is measured by each accelerometer(Crossbow, CX04LP1Z).

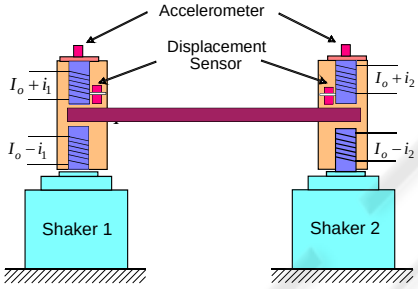

Figure 1: Schematic diagram of test rig

From the free-body diagram of the system in Fig. 3, the equation of motion is given by

$$\frac{m}{4}\begin{Bmatrix}\ddot{y}_1+\ddot{y}_2+\ddot{z}_1+\ddot{z}_2\\ \ddot{y}_1+\ddot{y}_2+\ddot{z}_1+\ddot{z}_2\end{Bmatrix}-\frac{J}{4a^2}\begin{Bmatrix}-\ddot{y}_1+\ddot{y}_2-\ddot{z}_1+\ddot{z}_2\\ \ddot{y}_1-\ddot{y}_2+\ddot{z}_1-\ddot{z}_2\end{Bmatrix}+\frac{mg}{2}\begin{Bmatrix}1\\1\end{Bmatrix}=\begin{Bmatrix}f_1\\f_2\end{Bmatrix} \quad (1)$$

where m and J are the mass and the mass moment of inertia about the mass center of the shaft. y, $\ddot{z}$ and f mean the air gap, the vertical acceleration and the actuating force, respectively. The subscripts 1 and 2 denote the positions of the AMB-1 and the AMB-2, respectively. This definition is consistent hereafter.

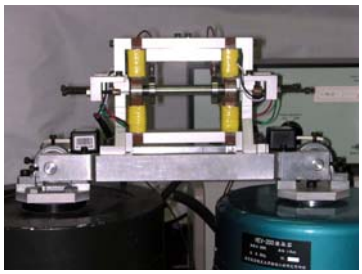

Figure 2: Photograph of test rig

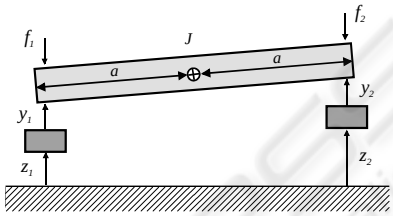

Figure 3: Free-body diagram of the levitated axis

The magnetic attractive force is approximately proportional to the square of the coil current and inversely proportional to the square of gap. However the nonlinearity of the magnetic attractive force against the coil current is decreased with the bias current added to the coil current. Consequently the linearized model is given by

$$f_c = K_d y + K_i i_c \quad (2)$$

where K_y is the displacement stiffness and K_i is the current stiffness.

Since the time constant of the power amplifier-magnet coil can be designed to be small enough by current feedback control, the control current i_c can be assumed to be proportional to the applied voltage, u_c, to the amplifier, i.e.

$$i_c = K_a u_c \quad (3)$$

where K_a is the gain of the amplifier.

Substituting eqs. (2) and (3) into eq. (1) gives the linearized AMB system model as follows:

$$\begin{Bmatrix}\ddot{y}_1\\ \ddot{y}_2\end{Bmatrix}-\frac{1}{mJ}\begin{bmatrix}K_{d1}(J+ma^2) & K_{d2}(J-ma^2)\\ K_{d1}(J-ma^2) & K_{d2}(J+ma^2)\end{bmatrix}\begin{Bmatrix}y_1\\y_2\end{Bmatrix} = \frac{K_a}{mJ}\begin{bmatrix}K_{i1}(J+ma^2) & K_{i2}(J-ma^2)\\ K_{i1}(J-ma^2) & K_{i2}(J+ma^2)\end{bmatrix}\begin{Bmatrix}u_1\\u_2\end{Bmatrix}-\begin{Bmatrix}\ddot{z}_1+g\\ \ddot{z}_2+g\end{Bmatrix} \quad (4)$$

It is clear from eq.(4) that the system is open-loop unstable, and the base acceleration and the gravitational force disturb the system.

3 CONTROLLER DESIGN

The system model in eq. (4) can be represented by the state space equation as

$$\dot{q} = Aq + Bu - d_a - f_g \tag{5}$$

$$q = \{y_1 \;\; y_2 \;\; \dot{y}_1 \;\; \dot{y}_2\}^T, \; u = \{u_1 \;\; u_2\}^T$$

$$d_a = [0 \;\; 0 \;\; \ddot{z}_1 \;\; \ddot{z}_2]^T, \; f_g = [0 \;\; 0 \;\; g \;\; g]^T \tag{6}$$

Since this system has no integrator, the state feedback control with integral is applied to eliminate the steady state error due to the gravity force.

$$u = -Kq - k_i \eta \tag{7}$$

where K and k_i are the state feedback gain vectors, and η is the integration of y_1 and y_2, i.e., $\dot{\eta} = \{y_1 \;\; y_2\}^T$.

The feedback gains in eq.(7) can be design from various kinds of schemes. The closed-loop system stabilized by eq. (7) can be represented in discrete time domain as

$$\begin{aligned} A_1(q^{-1})y_1(k) &= B_{11}(q^{-1})u_1(k) + B_{12}(q^{-1})u_2(k) \\ &\quad + C_{11}(q^{-1})d_1(k) + C_{12}(q^{-1})d_2(k) \\ A_2(q^{-1})y_2(k) &= B_{21}(q^{-1})u_1(k) + B_{22}(q^{-1})u_2(k) \\ &\quad + C_{21}(q^{-1})d_1(k) + C_{22}(q^{-1})d_2(k) \end{aligned} \tag{8}$$

where variables with the index k mean the sampled variables. $A_1(q^{-1})$, $B_{ij}(q^{-1})$ and $C_{ij}(q^{-1})$ are the system polynomials. q^{-1} is the one step delay operator.

A general compensator for the system in eq.(8) is defined by

$$\begin{aligned} u_1(k) &= W_{11}(q^{-1})d_1(k) + W_{12}(q^{-1})d_2(k) \\ u_2(k) &= W_{21}(q^{-1})d_1(k) + W_{22}(q^{-1})d_2(k) \end{aligned} \tag{9}$$

Applying the compensator, eq.(9), to the system, eq.(8), yields the compensated system of the form

$$\begin{aligned} A_1 y_1(k) &= [B_{11}W_{11} + B_{12}W_{21} + C_{11}]d_1(k) \\ &\quad + [B_{11}W_{12} + B_{12}W_{22} + C_{12}]d_2(k) \end{aligned}$$

$$\begin{aligned} A_2 y_2(k) &= [B_{21}W_{11} + B_{22}W_{21} + C_{21}]d_1(k) \\ &\quad + [B_{21}W_{12} + B_{22}W_{22} + C_{22}]d_2(k) \end{aligned} \tag{10}$$

Obviously, the perfect disturbance cancelling compensators W_{11}^*, W_{21}^*, W_{12}^*, W_{22}^* are derived from

$$\begin{Bmatrix} W_{11}^* \\ W_{21}^* \\ W_{12}^* \\ W_{22}^* \end{Bmatrix} = \frac{1}{B_{11}B_{22} - B_{12}B_{21}} \begin{Bmatrix} B_{22}C_{11} - B_{12}C_{21} \\ -B_{21}C_{11} + B_{11}C_{21} \\ B_{22}C_{12} - B_{12}C_{22} \\ -B_{21}C_{12} + B_{11}C_{22} \end{Bmatrix} \tag{11}$$

Since the compensators given in eq.(11) are designed from the system model, the compensation performance should be sensitive to the accuracy of the model. In practice, however, this kind of perfect cancelling based on the model is not expected because of the problems such as inaccuracy of dynamic model, approximation error of a discrete equivalent to a continuous transfer function, and sensor dynamics. Motivated by these problems, an explicit optimal feedforward compensator design technique is proposed in this paper. By this technique, the feedforward compensator design can be separated into two parts.

1) Disturbance cancelling control for single harmonic base motion

It is clear from eq. (11) that the response to a harmonic base motion of the frequency ω_r can be exactly nullified by choosing the polynomial $W_{ij}(q^{-1})$ as the first order polynomial satisfying the relation

$$\left[W_{ij} = w_{ij}^1 + w_{ij}^2 q^{-1} \right]_{q=e^{jw_rT}} = W_{ij}^*\Big|_{q=e^{jw_rT}}, \; i, j = 1, 2 \tag{12}$$

where T is the sampling interval.

Nullifying disturbance response by using feedforward compensator means physically matching the impedance from the base motion to the air-gap with the impedances from the base motions to the air-gaps through the AMB dynamics and of the feedforward compensators, so that the disturbance can be perfectly cancelled. However compensator design from the model is not suitable for practical applications. To get rid of the problems associated with the inaccurate model, adaptation of the feedforward compensator is proposed. This technique is an explicit design through experiments by using a multiple-FXLMS algorithm. The FXLMS algorithm has been extensively used in the field of active noise control(Kuo, 1996; Widrow and Stearns,

1985)). Figure 4 shows an example of the multiple-FXLMS algorithm to estimate the compensator polynomial W_{11}^* . The parameters of the compensators are estimated from the following update equation.

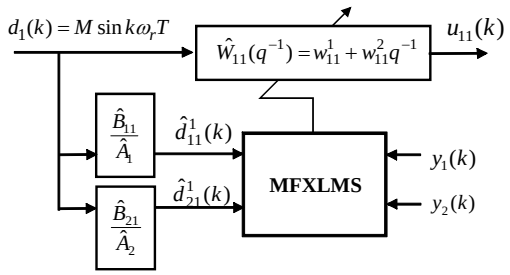

Figure 4: MFLMS algorithm for estimating $W_{11}(q^{-1})$

$$\begin{Bmatrix} w_{ij}^1(k+1) \\ w_{ij}^2(k+1) \end{Bmatrix} = \begin{Bmatrix} w_{ij}^1(k) \\ w_{ij}^2(k) \end{Bmatrix} + \mu_{ij} \frac{\begin{Bmatrix} \hat{d}_{1i}^j(k) \\ \hat{d}_{1i}^j(k-1) \end{Bmatrix}}{D_{1i}^j(k)} y_1(k) + \eta_{ij} \frac{\begin{Bmatrix} \hat{d}_{2i}^j(k) \\ \hat{d}_{2i}^j(k-1) \end{Bmatrix}}{D_{2i}^j(k)} y_2(k) \quad (13)$$

$$D_{ij}^m(k) = \hat{d}_{ij}^m(k)^2 + \hat{d}_{ij}^m(k-1)^2, \hat{d}_{ij}^m(k) = \frac{\hat{B}_{ij}}{\hat{A}_i} d_m(k),\ i, j, m = 1,2$$

where μ_{ij} and η_{ij} are the update gains, $\hat{A}_i(q^{-1})$ and $\hat{B}_{ij}(q^{-1})$ are the estimated system polynomials. All the compensator polynomials are estimated simultaneously from eq. (13).

By applying the MFXLMS algorithm meanwhile the exciters generate a stationary single harmonic base motion, the control parameters w_{ij}^1 and w_{ij}^2 in eq. (13) are estimated.

Since the base motion is single harmonic of frequency ω_r , the Fourier transforms $D_1(j\omega_r)$ and $D_2(j\omega_r)$ of d_1 and d_2 , respectively, would yield the relation $D_1(j\omega_r) = \alpha D_2(j\omega_r)$, where α is a complex number which represents the magnitude and phase relations between d_1 and d_2 . The estimated polynomials are not unique but satisfy two independent relations in the following

$$\alpha \begin{Bmatrix} \hat{W}_{11} \\ \hat{W}_{21} \end{Bmatrix} + \begin{Bmatrix} \hat{W}_{12} \\ \hat{W}_{22} \end{Bmatrix} = \alpha \begin{Bmatrix} W_{11}^* \\ W_{21}^* \end{Bmatrix} + \begin{Bmatrix} W_{12}^* \\ W_{22}^* \end{Bmatrix} = \begin{Bmatrix} \beta_1 \\ \beta_2 \end{Bmatrix} \quad (14)$$

Thus it is necessary to have at least two sets of polynomials estimated from the experiments where d_1 and d_2 have the same frequency but have different relations. For example, if a set of polynomials is estimated from the experiment where $\alpha = \alpha_1$ then one can determine β_1 and β_2 from eq.(14) as

$$\alpha_1 \begin{Bmatrix} \hat{W}_{11} \\ \hat{W}_{21} \end{Bmatrix} + \begin{Bmatrix} \hat{W}_{12} \\ \hat{W}_{22} \end{Bmatrix} = \begin{Bmatrix} \beta_1^1 \\ \beta_2^1 \end{Bmatrix} \quad (15)$$

Similarly, from another set of estimated polynomials obtained from another experiment where $\alpha = \alpha_2 \neq \alpha_1$, β_1 and β_2 are obtained as

$$\alpha_2 \begin{Bmatrix} \hat{W}_{11} \\ \hat{W}_{21} \end{Bmatrix} + \begin{Bmatrix} \hat{W}_{12} \\ \hat{W}_{22} \end{Bmatrix} = \begin{Bmatrix} \beta_1^2 \\ \beta_2^2 \end{Bmatrix} \quad (16)$$

From eqns. (14)-(16), the compensator polynomials that perfectly cancel any stationary harmonic base disturbance of the specified frequency ω_r can be determined as

$$\begin{Bmatrix} W_{11}^* \\ W_{21}^* \\ W_{12}^* \\ W_{22}^* \end{Bmatrix} = \begin{bmatrix} \alpha_1 & 0 & 1 & 0 \\ 0 & \alpha_1 & 0 & 1 \\ \alpha_2 & 0 & 1 & 0 \\ 0 & \alpha_2 & 0 & 1 \end{bmatrix}^{-1} \begin{Bmatrix} \beta_1^1 \\ \beta_2^1 \\ \beta_1^2 \\ \beta_2^2 \end{Bmatrix} \quad (17)$$

Repeating the above experimental procedures by changing the base motion frequency, sets of perfect cancelling compensator polynomials for each frequency are obtained.

2) Model fitting in frequency domain

From the sets of compensator parameters for each specified frequency, the FRF(frequency response function) of the disturbance cancelling feedforward compensators can be calculated. Based on this FRF, the compensators in eq. (9) are determined so as to minimize the cost function *J*

$$J_{ij} = \sum_{k=1}^{n} \lambda_{ij}(\omega_k) \left[\hat{W}_{ij}^*(q^{-1}) - W_{ij}(q^{-1}) \right]^2_{q=e^{j\omega_k T}},\ i, j = 1,2 \quad (18)$$

where $\lambda_{lm}(\omega_k)$ is the frequency weighting and $\hat{W}_{lm}^*(q^{-1})$ is the estimated compensator obtained in the first step and $W_{lm}(q^{-1})$ is the compensator to be determined. To avoid unstable compensator, $W_{lm}(q^{-1})$ can have the form of FIR(finite impulse response) filter.

4 EXPERIMENTS

To verify the effectiveness of the proposed control scheme, experiments were conducted using the test apparatus shown in Fig. 2. All control algorithms were implemented on a digital computer equipped with a DSP(TI-DS-1104)) board. Throughout the experiments, the sampling frequency was kept at 2000Hz.

A pole placement feedback (FB) control was designed to have a closed-loop system with a damping ratio of $\varsigma = 0.8$ and natural frequency of $\omega_n = 80Hz$ in consideration of the spectral characteristics of the base motion. The vehicle motion is characterized by a band-limited random process of bandwidth 15Hz-60Hz.

To evaluate the convergence of the estimated compensator parameters and the corresponding disturbance rejection performance, a sequence of simple harmonic of frequency 30Hz was delivered to the shakers. The resultant base motion kept the relation $D_1(j\omega) = 1.023 D_2(j\omega)$.

Figs. 5 and 6 show the estimated compensator parameters of $\hat{W}_{11}$ and the corresponding air-gap responses, respectively. We confirmed that all estimated parameters converged to their final values after 50 s. These figures reveal that the air-gap responses were consequently reduced, as the estimated parameters converged to their final values. The aforementioned convergence property and the disturbance rejection performance exhibit the feasibility of the proposed compensation control by means of the MFXLMS algorithm.

As explained in the above, at least, one more set of compensator parameters is necessary to determine the unique compensator polynomials which cancel the disturbance responses perfectly at $f = 30Hz$. The MFXLMS algorithm was applied to obtain another set of compensator parameters under the different base motion profile kept the relation $D_1(j\omega) = 1.465 e^{j\pi/2} D_2(j\omega)$, $f = 30Hz$. Similar convergence and disturbance rejection properties to Figs. 6 and 7 were confirmed.

From the two sets of the parameters obtained, the FRF of the disturbance neutralizing compensator at $f = 30Hz$ was determined. The disturbance rejection performance of this compensator was evaluated under the base motion yielding the relation $D_1(j\omega) = 0.69 e^{-j\pi/4} D_2(j\omega)$, $f = 30Hz$.

Fig. 7 shows the air-gap responses of the FB-control by itself and the FB with the compensation control. Fig. 7 reveals that the compensation control can almost neutralize any base motion responses of frequency 30Hz. Surprisingly, it was found that the control effort is reduced when the compensation was employed. The air-gap responses that remained after employing the compensation came mainly from the inability of the shakers to produce a pure sinusoidal tone of motion.

Repeating the experiment, while changing the harmonic base motion frequency, sets of disturbance neutralizing compensator parameters for each frequency were obtained. The FRF $\hat{W}_{11}$ calculated from the estimated parameters is shown as an example in Fig. 8. Based on the FRF in Fig. 8, the best-fit compensator was determined to be the third-order polynomials.

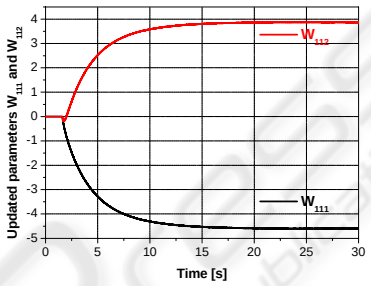

Figure 5: Estimated coefficients of $W_{11}(q^{-1})$.

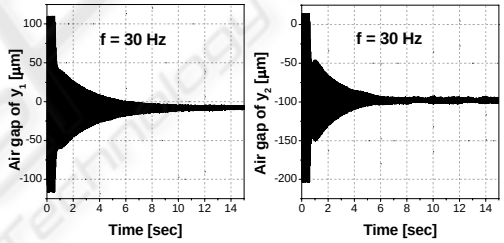

Figure 6: Air-gap responses during estimation by MFXLMS algorithm

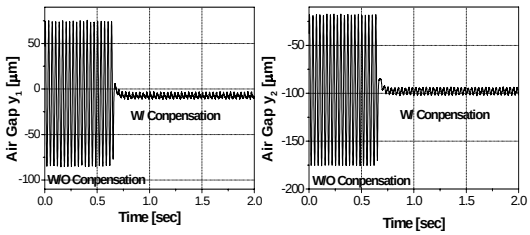

Figure 7: Compensated air gap responses

To investigate the efficiency of the designed compensator, a comparison was made between the air-gap response with the compensation and without the compensation. During the control experiments, a sequence of band-limited random signals of bandwidth 15-60Hz was delivered to the shaker and the resultant base motion resembled that of the real vehicle.

As shown in Fig. 9, the air-gap responses were greatly reduced by applying the feedforward

compensation. For y_1, the standard deviations of the air-gap with compensation and without compensation were calculated to be $\sigma = 14.53\mu m$ and $1.43\mu m$, respectively. For y_2, the standard deviations of the air-gap with compensation and without compensation were calculated to be $\sigma = 13.13\mu m$ and $1.08\mu m$, respectively. The control voltages were slightly reduced after employing compensation. Figure 10 shows the spectra of the air-gap responses in Fig. 9. The disturbance attenuation ratio is approximately–20db within the frequency band of the base motion.

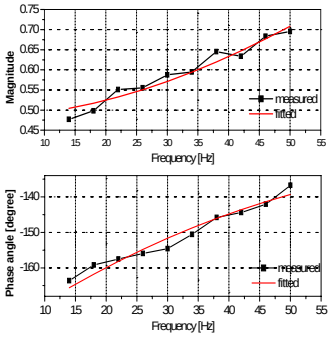

Figure 8: Measured and fitted FRF of $\hat{W}_{11}$

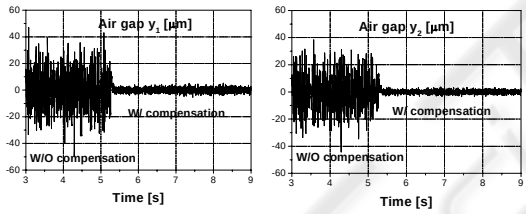

Figure 9: Air-gap responses w/ and w/o compensation

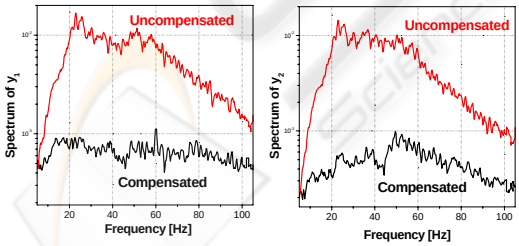

Figure 10: Spectra of air-gap with and without compensation

5 CONCLUSION

In this work, an experimental feedforward compensator design technique, developed from an adaptive estimation by means of the Multiple Filtered-x least mean square (MFXLMS) algorithm has been proposed. The feasibility of the proposed technique has been verified by an experimental study, by using a 2-DOF active magnetic bearing system subject to base motion. The experimental results showed that the standard deviation of the compensated response was reduced to less than 10% of that by feedback control alone.

ACKNOWLEDGEMENT

This work was supported by grant no.(R01-2003-000-10857-0) from the Basic Research Program of the Korea Science & Engineering Foundation.

REFERENCES

Brunet, M., 1998. Practical Applications of Active Magnetic Bearing to the Industrial World. *1'st International Symposium on Magnetic Bearing*. Zurich, pp.225-244.

Cole, M. O. T., Keogh, P. S. and Burrows, C. R. , 1998. Control and Non-linear Compensation of a Rotor/Magnetic Bearing System Subject to base Motion. *6th Int. Symposium on Magnetic Bearings*. Cambridge, MA, pp.618-627.

Jinzenji, A., Sasamoto, T., Aikawa, K., Yoshida, S. and Aruga, K., 2001. Acceleration feedforward control Against Rotational Disturbance in hard Disk Drives. *IEEE Trans. On Magnetics*. Vol.37, No.2, pp.888-893,.

Kasada, M.E., Clements, J., Wicks, A. L., Hall, C. D., and Kirk, R. G., 2000, Effect of sinusoidal base motion on a magnetic bearing, *Proc. IEEE International Conference on Control Applications*, pp.144-149.

Kuo, S. M. and Morgan, D. R., 1996. *Active Noise Control Systems*. A Wiley-Interscience Publication, John Wiley Sons, Inc.

Suzuki, Y., 1998. Acceleration Feedforward Control for Active Magnetic Bearing Excited by Ground Motion. *IEEE Proc. Control Theory Appl.* Vol.145, pp. 113-118.

Wang, A.K. and Ren, W., 1999, Convergence analysis of the multiple-variable filtered-x LMS algorithm with application to active noise control, *IEEE Trans. On Signal Processing*, Vol.47, No.4, pp.1166-1169.

White, M. T. and Tomizuka, M., 1997. Increased Disturbance Rejection in Magnetic Disk Drives by Acceleration Feedforward Control and Parameter Adaptation. *Control Engineering Practice*. vol.5, no.6., pp.741-751.

Widrow, B. and Stearns, S. D., 1985. *Adaptive Signal Processing*. Prentice Hall. Englewood Cliffs, NJ.